Am J Physiol Cell Physiol 283: C960–C970, 2002.
First published May 29, 2002; 10.1152/ajpcell.00163.2002.

Virtual cloning, functional expression, and gating analysis of human connexin31.9

THOMAS W. WHITE,[1] MIDUTURU SRINIVAS,[2] HARRIS RIPPS,[3]
ANGELA TROVATO-SALINARO,[4] DANIELE F. CONDORELLI,[4] AND ROBERTO BRUZZONE[5]
[1]*Department of Physiology and Biophysics, State University of New York, Stony Brook, 11794-8661;*
[2]*Department of Neuroscience, Albert Einstein College of Medicine, Bronx, New York 10461;*
[3]*Department of Ophthalmology and Visual Sciences, University of Illinois at Chicago College of Medicine, Chicago, Illinois 60612;* [4]*Department of Chemical Sciences, University of Catania, 95125 Catania, Italy; and* [5]*Department of Neuroscience, Institut Pasteur, 75015 Paris, France*

Received 10 April 2002; accepted in final form 14 May 2002

White, Thomas W., Miduturu Srinivas, Harris Ripps, Angela Trovato-Salinaro, Daniele F. Condorelli, and Roberto Bruzzone. Virtual cloning, functional expression, and gating analysis of human connexin31.9. *Am J Physiol Cell Physiol* 283: C960–C970, 2002. First published May 29, 2002; 10.1152/ajpcell.00163.2002.—We have identified a novel gap junction gene by searching the human genome sequence database that encodes a protein designated as connexin31.9 (Cx31.9). Cx31.9 was most homologous to human Cx32.4 and did not cluster with either the purported α- or β-connexin subfamilies. Expression of Cx31.9 was detected by RT-PCR in human mRNA from several tissues including cerebral cortex, heart, liver, lung, kidney, spleen, and testis. A partial Cx31.9 sequence was also represented in the human Expressed Sequence Tag database. Cx31.9 formed intercellular channels in both paired *Xenopus* oocytes and transfected neuroblastoma N2A cells that were distinguished by an apparent low unitary conductance (12–15 pS) and a remarkable insensitivity to transjunctional voltage. In contrast, Cx31.9 channels were gated by cytoplasmic acidification or exposure to halothane like other connexins. Cx31.9 was able to form heterotypic channels with the highly voltage-sensitive *Xenopus* Cx38 (XenCx38), which provides an opportunity to study gating in heterotypic channels formed by hemichannels (connexons) composed of connexins with widely divergent properties. Thus Cx31.9 is a novel human connexin that forms channels with unique functional properties.

gene family; expression; channel; gap junction

CONNEXINS ARE THE PROTEIN subunits of intercellular channels that constitute vertebrate gap junctions (3). Although gap junctions are ubiquitously found between virtually all cells in contact, they are composed of different connexin isoforms in different tissues. Because intercellular channels require the participation of two neighboring cells, it is possible for each cell to contribute different connexin proteins, thereby increasing the potential for functional diversity (37). A wealth of in vitro expression studies has demonstrated that each type of connexin channel is endowed with distinctive functional properties, which in turn are derived from the unique primary sequences of the constituent connexins (8, 14). Thus whereas the term intercellular communication is widely used to describe gap junction-dependent intercellular signaling, the precise nature of the signals that are exchanged between cells is dictated by the complement of expressed connexins (6). The in vivo significance of this diversity of communication possibilities remains enigmatic, although studies of genetically engineered mice have demonstrated that connexin isoforms are not simply redundant. Targeted deletion of all connexins to date has always resulted in detectable phenotypic changes, although they were often unexpected (14, 26, 40). Furthermore, targeted replacement of connexin genes with different family members in mice has provided a direct demonstration that intrinsic functional properties of unique connexins are required for normal tissue function (24, 36). Taken together, these observations strongly argue that a complete understanding of gap junctional intercellular communication will require documentation of differences in the functional properties of the various connexin isoforms.

It is difficult to envision the complex range of intercellular communication behaviors that are available within any given tissue unless the full connexin complement of its component cells is unambiguously defined. As a prerequisite to this, the identification of all the connexin genes within a given organism's genome is required. The recent completion of the human genome sequencing project makes it possible to seek out and characterize all of the human gap junction genes. In the case of connexins, this search is greatly facilitated by the documented absence of introns within the open reading frame of the majority of connexin genes with the exception of connexin36 (Cx36) and connexin40.1 (2, 22; unpublished results).

Address for reprint requests and other correspondence: T. W. White, Dept. of Physiology and Biophysics, State Univ. of New York, T5-147, Basic Science Tower, Stony Brook, NY 11794-8661 (E-mail: thomas.white@sunysb.edu).

The costs of publication of this article were defrayed in part by the payment of page charges. The article must therefore be hereby marked "*advertisement*" in accordance with 18 U.S.C. Section 1734 solely to indicate this fact.

In this study, we have combined in silico cloning with standard molecular biological techniques to identify a novel connexin sequence in the human genome database that encodes connexin31.9 (Cx31.9). Cx31.9 was most highly related to connexin32.4 (Cx32.4) and clustered on the third non-α/non-β branch of the connexin family tree. Cx31.9 mRNA was expressed in a variety of tissues and cell types including cerebral cortex, liver, spleen, and kidney. Cx31.9 mRNA was also represented in silico in the human Expressed Sequence Tag (EST) database. Functional characterization of Cx31.9 demonstrated its channel-forming ability in two different in vitro expression assays. In both assay systems, Cx31.9 channels showed a remarkable insensitivity to voltage-dependent gating, although the channels displayed normal sensitivity to chemically induced gating. Thus Cx31.9 is a bona fide member of the human connexin gene family in that it forms intercellular channels with unique functional properties.

MATERIALS AND METHODS

Molecular cloning of Cx31.9. A BLAST search in the National Center for Biotechnology Information (NCBI, National Library of Medicine, National Institutes of Health) High-Throughput Genome Sequences database yielded a *Homo sapiens* clone that, contained the intronless open reading frame of a new connexin with a predicted molecular mass of 31.9 kDa. A DNA fragment encompassing the coding sequence of Cx31.9 was amplified from human genomic DNA by PCR using primers corresponding to nucleotides 1–21 (sense: 5′-gatgatGGATCC-atgggggagtgggcgttcctg-3′) and 885–865 (antisense: 5′-tagtagTCTAGA-ctagatggccagatctcggcg-3′) that contained *Bam*HI (sense) and *Xba*I (antisense) linkers (capital letters). PCR products were purified using Qiaquick columns (Qiagen, Germantown, MD), digested with *Bam*HI/*Xba*I (Roche Molecular Biochemicals, Indianapolis, IN), purified by agarose gel electrophoresis, subcloned into the corresponding sites of the pCS2+ expression vector (31), and sequenced on both strands. Pairwise alignment of the translated amino acid sequence of Cx31.9 with 19 other human connexin sequences available in the NCBI database at the time of writing was performed using MegAlign software (DNASTAR, Madison, WI).

RT-PCR analysis of Cx31.9 expression. Human central nervous system tissues (spinal cord, medulla oblongata, cerebellum, striatum, hippocampus, and neocortex) were obtained at autopsy from a 26-yr-old male, frozen in dry ice-cooled isopentane, and stored at −80°C before total RNA extraction. Additional human total RNAs were commercially obtained from Ambion (Austin, TX). Total RNA (5 μg) was reverse transcribed with 150 ng of random hexamers and 200 units of RNase H^- RT (SuperScript II Invitrogen, Life Technologies, Carlsbad, CA) in a reaction mixture that contained 20 mM Tris·HCl (pH 8.4 at 25°C), 50 mM KCl, 5 mM $MgCl_2$, 0.5 mM dNTP mix, 0.01 M dithiothreitol, and 40 units of the recombinant RNase inhibitor RNaseOUT (Invitrogen). Samples were incubated at 25°C for 10 min and then at 42°C for 50 min. The reaction was terminated by 15 min of incubation at 70°C. After cooling the samples in ice, 1 μl (2 units) of RNase H^- RT was added, and the samples were incubated at 37°C for 20 min. To exclude the significant contribution of genomic DNA to the final PCR step, incubations with or without RT (RT+ and RT−, respectively) were run simultaneously for each RNA sample. Only RNA samples with RT− reactions that did not provide detectable PCR amplification products were included in the results.

PCR for detection of Cx31.9 (HCx31.9) mRNA was performed by using 25 pmol of primers and 1 μl of cDNA in a reaction mixture that contained 20 mM Tris·HCl (pH 8.4), 50 mM KCl, 1.5 mM $MgSO_4$, 0.2 mM dNTP, 2× PCRx Enhancer System (Invitrogen), and 2.5 units of Platinum *Taq* DNA polymerase (Invitrogen). After an initial denaturation at 95°C for 3 min, 30 cycles of amplification with a Perkin-Elmer 480 thermocycler were performed under the following conditions: 95°C for 1 min, 60°C for 2 min, and 72°C for 3 min. Sense: 5′-CAGCGCCATGGGGGAGTGGG-3′ and antisense: 5′-CCCTAGATGGCCAGATCTCG-3′ primers were used for amplification of the entire 894-bp coding region of HCx31.9. To control for the quality of the reverse transcription reaction, cDNA samples were also amplified with β-actin primers (sense: 5′-TGACGGGGTCACCCACACTGTGCCCATCTA-3′ and antisense: 5′-CTAGAAGCATTGCGGTGGACGATGGAGGG-3′). PCR was performed using 25 pmol of primers, 1 μl of cDNA, and 2.5 units of Platinum *Taq* DNA polymerase in a standard reaction mixture that contained (in mM) 20 Tris·HCl (pH 8.4), 50 KCl, 1.5 $MgCl_2$, and 0.2 dNTP. A denaturation step at 95°C for 3 min was followed by 25 amplification cycles (95°C for 1 min, 64°C for 2 min, and 68°C for 1 min). Amplification products were separated by agarose gel electrophoresis and visualized with ethidium bromide. To confirm the identity of amplified products, DNA fragments were recovered from agarose gel with the GeneClean II Kit (Bio 101 Systems), subcloned in pPCR-Script SK(+) (Stratagene), and sequenced by the fluorescent dideoxy chain-termination procedure with the ABI Prism 377 automatic sequencer.

In vitro transcription, oocyte microinjection, and pairing. Cx31.9 in the pCS2+ plasmid was linearized with *Apa*I, gel purified, and used as template (1 μg of DNA) to produce capped RNA using the mMessage mMachine kit (Ambion). The purity and yield of transcribed cRNA was determined by measuring absorbance at 260/280 nm. *Stage V-VI* oocytes were collected from adult *Xenopus laevis* females (Nasco, Fort Atkinson, WI) following previously described protocols (7). Oocytes were isolated and defolliculated by enzymatic digestion and were cultured in modified Barth's (MB) medium at 18°C. For physiological analysis, cells were injected with a total volume of 40 μl of either an antisense oligonucleotide (3 ng/cell) to suppress the endogenous *Xenopus* connexin38 (XenCx38) or a mixture of the antisense oligonucleotide plus Cx31.9 RNA (40 ng/cell) using a Nanoject II Auto-Nanoliter oocyte injector (Drummond, Broomall, PA). Where specified, oocytes were mock treated with an identical volume of water to determine the ability of Cx31.9 to interact with endogenous XenCx38. After an overnight incubation at 18°C, microinjected oocytes were immersed for a few minutes in hypertonic solution to strip the vitelline envelope (21), transferred to petri dishes containing MB medium, and manually paired with vegetal poles apposed.

Electrical recordings from oocytes. The functional properties of cell-to-cell channels were assessed by a dual voltage-clamp procedure that enabled direct quantitation of junctional conductance (29). Current and voltage electrodes (1.2-mm diameter, Glass of America, Millville, NJ) were pulled to a resistance of 1–2 MΩ with a horizontal puller (Narishige, Tokyo, Japan) and filled with a solution containing 3 M KCl, 10 mM EGTA, and 10 mM HEPES, pH 7.4. Voltage clamping of oocyte pairs was performed using two GeneClamp 500 amplifiers (Axon Instruments, Foster City, CA) controlled by a PC-compatible computer through a Digidata 1320A interface (Axon Instruments). pCLAMP 8.0 software (Axon In-

struments) was used to program stimulus and data collection paradigms. Current outputs were filtered at 50 Hz and the sampling interval was 10 ms. For simple measurements of junctional conductance, both cells of a pair were initially clamped at −40 mV to ensure zero transjunctional potential (V_j) and alternating pulses of ±10–20 mV were imposed to one cell. Current delivered to the cell clamped at −40 mV during the voltage pulse was equal in magnitude to the junctional current (I_j) and was divided by the voltage to yield the conductance.

To determine the voltage-gating properties of Cx31.9, V_j values of opposite polarity were generated by hyperpolarizing or depolarizing one cell in 20-mV steps (over a range of ±100–120 mV) while clamping the second cell at −40 mV. In some experiments, cells were initially clamped at −90 mV and depolarizing voltage steps were applied to one cell of the pair in 30-mV increments up to +90 mV (final V_j = 180 mV). Currents were measured 4 s after the onset of the voltage pulse, at which time they approached steady state (I_{jss}), and the macroscopic conductance (G_{jss}) was calculated by dividing I_{jss} by V_j. G_{jss} was then normalized to the values determined at ±20 mV and plotted against V_j. Data describing the relationship of G_{jss} as a function of V_j were analyzed using Origin 5.0 (Microcal Software, Northampton, MA) and fit to a Boltzmann relation of the form $G_{jss} = \{(G_{jmax} - G_{jmin})/1 + \exp[A(V_j - V_0)]\} + G_{jmin}$, where G_{jss} is the steady-state junctional conductance, G_{jmax} (normalized to unity) is the maximum conductance, G_{jmin} is the residual conductance at large values of V_j, and V_0 is the V_j at which $G_{jss} = (G_{jmax} - G_{jmin})/2$. The constant A ($A = nq/kT$) represents the voltage sensitivity in terms of gating charge as the equivalent number (n) of electron charges (q) moving through the membrane, k is the Boltzmann constant, and T is the absolute temperature. The average conductance of oocyte pairs selected for analysis of voltage sensitivity was well below 5 μS, which thereby ensured adequate control of V_j and avoided the risk of overestimating the actual G_j value at steady state (42).

The time constants (τ) of voltage-dependent transitions of junctional conductance were determined for the XenCx38 homotypic channels and for the XenCx38 side of the Cx31.9/XenCx38 heterotypic oocyte pairs using data-fitting functions in Origin 5.0 software. Experimental τ values were calculated for V_j values ≥80 mV, which resulted in comparable levels of G_{jss} irrespective of whether XenCx38 was paired in a homotypic or heterotypic fashion.

The effect of intracellular proton concentration (pH_i) on junctional conductance was tested on paired oocytes that expressed Cx31.9 or XenCx38. After a 2-min equilibration period, the incubation dish (total volume = 6 ml) was perfused for 4 min with MB solution saturated with 100% carbon dioxide at a flow rate of 4 ml/min, after which the perfusion medium was switched back to normal MB to allow junctional conductance to recover. Although no attempt was made to determine the precise levels of pH_i under these conditions, measurements with both pH-sensitive microelectrodes and proton-sensitive dyes indicate that in oocytes, this procedure typically induces a rapid intracellular acidification in excess of 1 pH unit (12, 34). I_j values were recorded (sampling interval = 40 ms, output filter = 10 Hz) in response to alternating pulses (±40 mV for Cx31.9 and ± 10 mV in the case of XenCx38), applied to one cell for 1 s at 20-s intervals, and normalized to the average conductance values recorded during the first minute of equilibration.

Functional expression of Cx31.9 in transfected N2A cells. N2A cells were cotransfected with Cx31.9 cDNA and enhanced green fluorescent protein (EGFP) cDNA in separate vectors using the Lipofectamine 2000 reagent (GIBCO-BRL, Gaithersburg, MD) following previously described procedures (16). Transiently transfected cells were dissociated 8–12 h after transfection and plated at low density on 1-cm glass coverslips. Cell cultures were maintained in a 37°C incubator in a moist 5% CO_2-95% air environment. Cx31.9-expressing cell pairs were identified by the fluorescent emission of EGFP (excitation, 488 nm; emission, >520 nm) using a Nikon Diaphot microscope equipped with a xenon arc lamp. Junctional conductance was measured between cell pairs by using the dual whole cell voltage-clamp technique with Axopatch 1C or 1D patch-clamp amplifiers (Axon Instruments) at room temperature. The solution bathing the cells contained (in mM) 140 NaCl, 5 KCl, 2 CsCl, 2 $CaCl_2$, 1 $MgCl_2$, 5 HEPES, 5 dextrose, 2 pyruvate, and 1 $BaCl_2$; pH 7.4. Patch electrodes had resistances of 3–5 MΩ when filled with internal solution that contained (in mM) 130 CsCl, 10 EGTA, 0.5 $CaCl_2$, 3 Mg-ATP, 2 Na_2-ATP, and 10 HEPES; pH 7.2. Current recordings were filtered at 0.2–0.5 kHz and sampled at 1–2 kHz. Data were acquired using pCLAMP 8.0 software and analyzed with either pCLAMP 8.0 or Origin 6.0 software. Each cell of a pair was initially held at a common holding potential of 0 mV. To evaluate junctional coupling, hyperpolarizing pulses to various voltages were applied to one cell to establish a V_j gradient, and I_j was measured in the second cell (held at 0 mV). Single-channel currents were investigated in weakly coupled cell pairs by applying −140- or −160-mV pulses to one cell of a pair.

Statistical analysis. Results are shown as means ± SE. Comparisons between two populations of data were made with Student's unpaired t-test; P values of 0.05 or less were considered to be significant.

RESULTS

Sequence analysis and tissue distribution of Cx31.9. We initially identified Cx31.9 from BLAST software searches of human DNA sequences in the NCBI High-Throughput Genome Sequence database. A putative connexin open reading frame with a predicted molecular mass of 31.932 kDa (thus Cx31.9) was found in the chromosome 17 draft sequence (GenBank accession no. AC018629, AF514298). Comparison of the full-length Cx31.9 amino acid sequence with 19 other human connexin sequences showed a threshold of 30–40% overall sequence identity (Fig. 1*A*), which confirms its membership in the connexin family of gap junction proteins. Only connexin Cx32.4 (GenBank accession no. XM064450) showed notable amino acid identity with Cx31.9 (76%), and an alignment of these two proteins is shown in Fig. 1*B*. Cx31.9 has all of the predicted features of a typical connexin including four transmembrane domains, cytoplasmic amino and carboxy termini, and the conserved cysteines at three positions in each of the two extracellular loops. One unusual feature of Cx31.9 was the relatively high content of proline in its amino acid composition (33 of 294 amino acids) including a continuous sequence of 10 prolines in one region of the carboxy terminus. Alignment of a truncated Cx31.9 sequence, which lacks the highly divergent carboxy terminus, with other truncated human connexins revealed that it did not cluster within either the α- or β-connexin subgroups, which

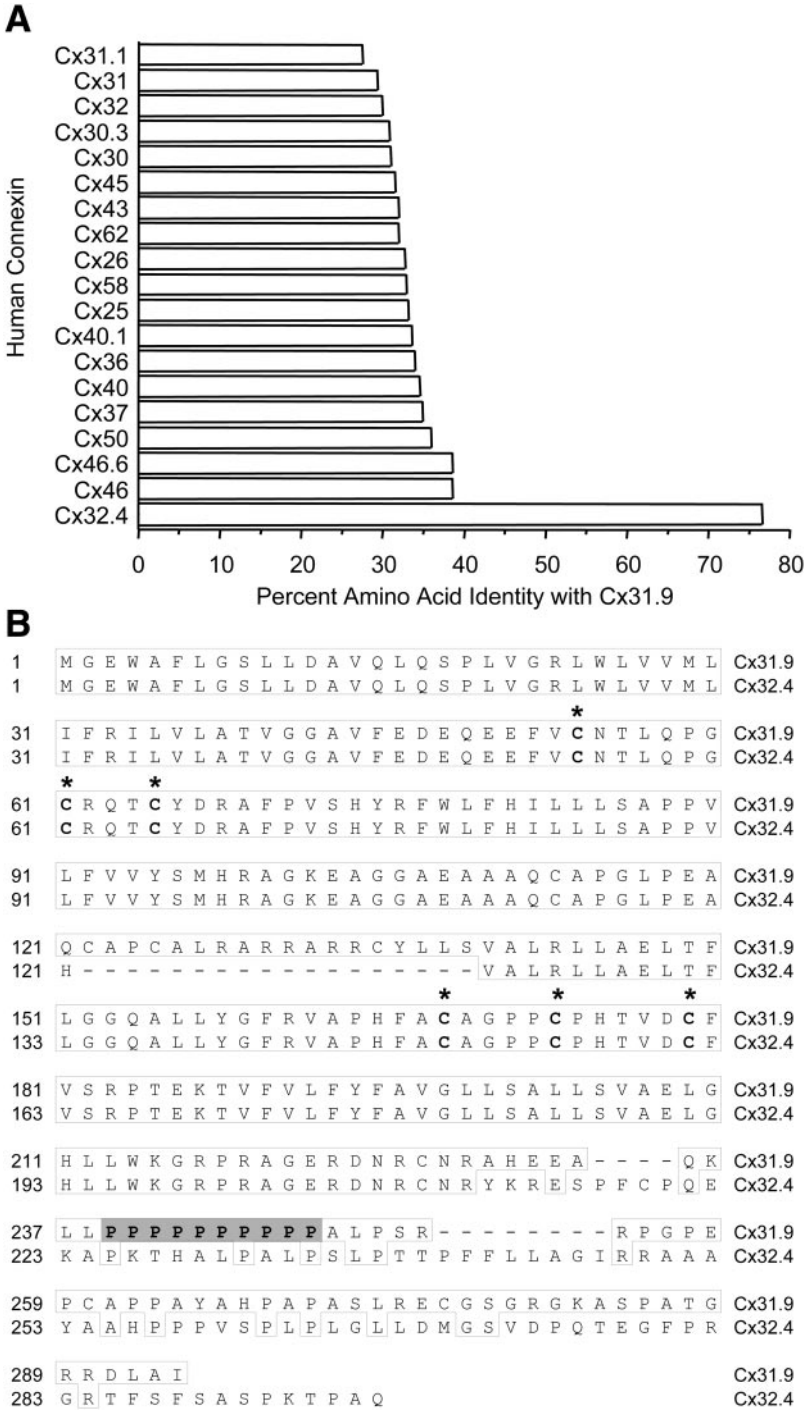

Fig. 1. Sequence analysis of connexin31.9 (Cx31.9). *A*: amino acid identity derived from pairwise sequence alignment of 19 human connexins with Cx31.9. Only connexin32.4 (Cx32.4) showed an overall identity >30–40% threshold common to all connexins. *B*: amino acid sequence alignment of Cx31.9 with Cx32.4 created with the ClustalW program (30): dashes indicate gaps, dotted lines surround residues identical to Cx31.9, and * show three conserved cysteines in each extracellular loop. Presence of a proline-rich region in the carboxy terminal domain is a distinctive feature of Cx31.9 (shaded area). Amino terminus, transmembrane domains, and extracellular loops are identical between Cx31.9 and Cx32.4, whereas the central cytoplasmic loop and carboxy terminus differ. Predicted features of Cx31.9 are consistent with other known connexins.

suggests that it may belong to a new clade that includes Cx32.4 and several other outlying connexins (Fig. 2).

To exclude the possibility that Cx31.9 represented a pseudogene, we ascertained whether its coding sequence was actually transcribed into mRNA. Expression of Cx31.9 was analyzed by RT-PCR of human RNA isolated from different tissues (Fig. 3). Cx31.9 transcripts were detected in human liver, heart, spleen, lung, kidney, testis, ovary, adrenal gland, cerebral cortex, and hippocampus. Inconclusive or negative Cx31.9 signals were obtained when human RNAs from pancreas, inferior olive, medulla oblongata, cerebellum, striatum, or spinal cord were used for RT-PCR analysis despite easy amplification of β-actin from these samples. In addition, BLAST searches of the NCBI human EST database revealed an EST sequence derived from human senescent fibroblasts that exactly matched nucleotides 411–840 of Cx31.9 (corresponding to amino acids 137–280, GenBank accession no. AI142991). These data verify that Cx31.9 was transcribed in a variety of tissues.

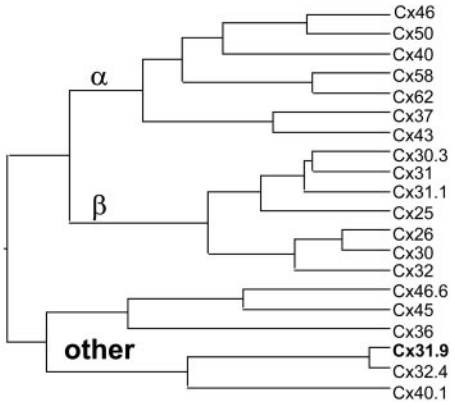

Fig. 2. Dendrogram of human connexin protein sequences. Sequences from Fig. 1*A* were truncated at the predicted end of the fourth transmembrane domain to eliminate the highly divergent carboxy termini. Connexins are equally distributed into three broad subgroups: the two previously described Greek groups as well as a third clade more divergent from the α- and β-connexins than the divergence between the α- and β-subgroups. Cx31.9 clusters in this non-Greek group with greatest homologies to Cx32.4 and connexin40.1 (Cx40.1).

Functional expression in Xenopus oocytes and N2A cells. The ability of Cx31.9 to form gap junction channels was tested in two different experimental systems, *Xenopus* oocytes and N2A cells (27, 32). To determine the functional characteristics of Cx31.9 in paired oocytes, cells were injected with 40 ng of in vitro transcribed cRNA and were manually paired after removal of the vitelline envelope. Oocytes were also injected with antisense oligonucleotides, against XenCx38 to minimize the contribution of this endogenous connexin to the recorded conductance (27). Cx31.9 consistently induced the assembly of intercellular channels that resulted in levels of gap junctional conductance that were an order of magnitude greater than those measured in antisense-treated control pairs (Fig. 4*A*, 0.54 ± 0.12 vs. 0.03 ± 0.03 μS; $P \leq 0.0001$, Student's unpaired *t*-test) albeit of a lower amplitude than those obtained with other mammalian connexins in this expression system (1, 27, 41). In addition, we examined the possibility that the human connexin could interact with endogenous XenCx38 by constructing heterotypic pairs between oocytes injected with Cx31.9 and mock-treated cells that did not receive antisense Cx38 oligonucleotides. Cx31.9/water pairs developed junctional conductance values that were greatly suppressed by injection of the antisense oligonucleotides, thus demonstrating the ability of Cx31.9 to recruit endogenous XenCx38 (Fig. 4*A*). The conductance measurements of these heterotypic pairs were of a magnitude similar to those of homotypic Cx31.9 pairs.

The ability of Cx31.9 to form gap junction channels in mammalian cells was determined by dual whole cell patch-clamp analysis after transient transfection of N2A cells with the Cx31.9 in pCS2+ plasmid. Recordings from cell pairs expressing Cx31.9 revealed conductance values 50-fold higher than those obtained from mock-transfected N2A cell pairs (Fig. 4*B*, 2.82 ± 0.71 vs. 0.05 ± 0.02 nS; $P \leq 0.002$). Therefore, Cx31.9

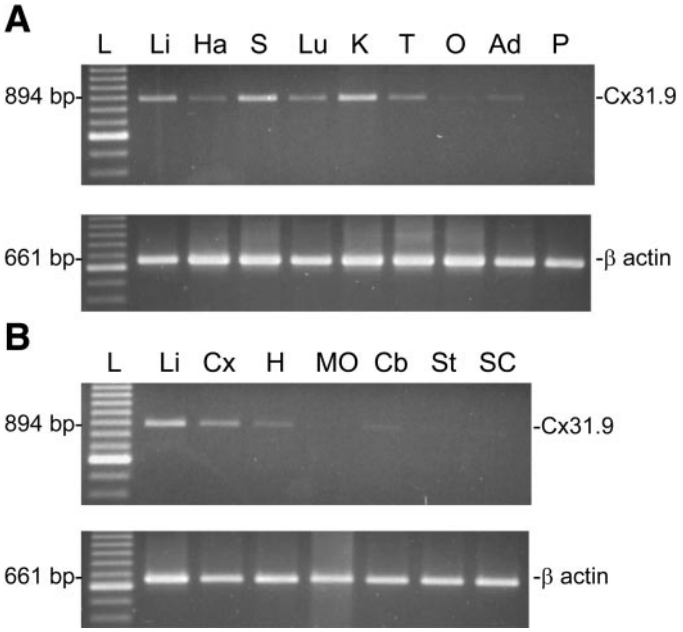

Fig. 3. Expression of Cx31.9 mRNA in different human organs (*A*) and brain regions (*B*) detected by RT-PCR. Expected Cx31.9 amplicon of 894 bp was not observed when RT was omitted from the reaction mixture (see MATERIALS AND METHODS). Each cDNA sample was also amplified with specific primers for the β-actin transcript (661-bp amplicon) as a control for the quality of the cDNA preparation. Molecular identity of the Cx31.9 bands was confirmed by sequencing. L, 100-bp ladder; Li, liver; Ha, heart; S, spleen; Lu, lung; K, kidney; T, testis; O, ovary; Ad, adrenal gland; P, pancreas; Cx, cerebral cortex; H, hippocampus; MO, medulla oblongata; Cb, cerebellum; St, striatum; and SC, spinal cord.

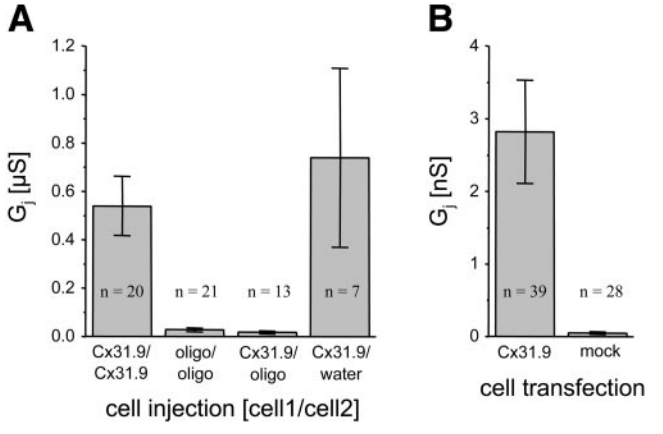

Fig. 4. Cx31.9 forms homotypic and heterotypic gap junction channels. *A*: oocytes pretreated with an oligonucleotide antisense to a sequence within the coding region of *Xenopus* connexin38 (XenCx38) were injected with either cRNA (Cx31.9) or vehicle (oligo) and paired for 24–48 h before junctional conductance (G_j) was measured by dual voltage clamp. To determine whether Cx31.9 could interact with the endogenous XenCx38, we constructed heterotypic pairs between antisense-treated oocytes injected with Cx31.9 cRNA and mock-treated cells that did not receive antisense XenCx38 oligonucleotides (water). Values are means ± SE of the indicated number of oocyte pairs. *B*: neuroblastoma N2A cells were transiently cotransfected with Cx31.9 and enhanced green fluorescent protein (EGFP) or were mock treated. G_j was measured between cell pairs using the dual whole cell voltage-clamp technique. Values are means ± SE of the indicated number of N2A cell pairs.

formed functional gap junction channels in two well-characterized in vitro expression systems, which demonstrates that it is a functional member of the human connexin family and allows for experimental determination of its physiological and pharmacological gating characteristics.

Voltage-gating behavior of Cx31.9. To characterize the physiological behavior of channels composed of Cx31.9, we first analyzed voltage dependence. N2A cells transiently transfected with Cx31.9 developed junctional conductance values that exhibited an absence of detectable voltage-dependent channel closure. A representative family of I_js evoked by voltage steps of opposite polarities and increasing amplitude shows that I_j did not decrease with time for V_j values up to ±100 mV (Fig. 5*A*). This property is unique to Cx31.9, as no other connexin has previously been shown to be voltage insensitive within this physiological range of V_j. Quantification of this unusual voltage-gating behavior by plotting normalized conductance (G_j) versus V_j demonstrated that even at the highest V_j values tested (±100 mV), Cx31.9 conductance remained insensitive to voltage in N2A cells (Fig. 5*B*). To ensure that this unusual property was not related to the choice of the host cell, we also examined Cx31.9 voltage gating in paired oocytes. Similar to N2A cells, plots of G_j versus V_j in oocyte pairs showed a complete lack of sensitivity to voltage at V_j values of ±100 mV (Fig. 5*C*). Because these findings did not rule out the possibility that Cx31.9 may be endowed with an exquisitely high voltage-gating threshold, we next performed a limited series of experiments in which depolarizing steps of up to +180 mV of V_j were imposed from a holding potential of −90 mV. This protocol showed that when the driving force was increased to supraphysiological values, Cx31.9 channels began to exhibit a very modest degree of voltage-dependent current decay (13 and 20% reduction in I_j at 150 and 180 mV, respectively, τ = 0.49 s at 180 mV, Fig. 5*D*). These data indicate that Cx31.9 formed intercellular channels that were completely voltage insensitive at V_j values of either polarity ≤120 mV.

Pharmacological inhibition of Cx31.9 channels. The striking absence of voltage gating in Cx31.9 channels led us to investigate whether these channels were sensitive to chemical gating induced by intracellular acidification or exposure to volatile anesthetics. The pH sensitivity of Cx31.9 intercellular channels was tested by perfusing oocyte pairs with MB that had been saturated with 100% CO_2, a procedure that typically induces a rapid cytoplasmic acidification in excess of 1 pH unit (12, 34). Intracellular acidification triggered a rapid fall in junctional conductance between oocyte pairs expressing Cx31.9 (>80% closure, Fig. 6*A*), which slowly recovered when the superfusate was switched back to normal MB. Conductance between pairs of Cx31.9-expressing oocytes was unaffected by switching superfusates when no change in pH was introduced (data not shown). Sensitivity of Cx31.9 conductance to the gap junction channel blocker halothane was determined in N2A cells. Application of halothane has been shown to produce rapid and reversible decreases in gap junctional conductance in a wide variety of mammalian cell lines (9, 25). Figure 6*B* shows a series of intercel-

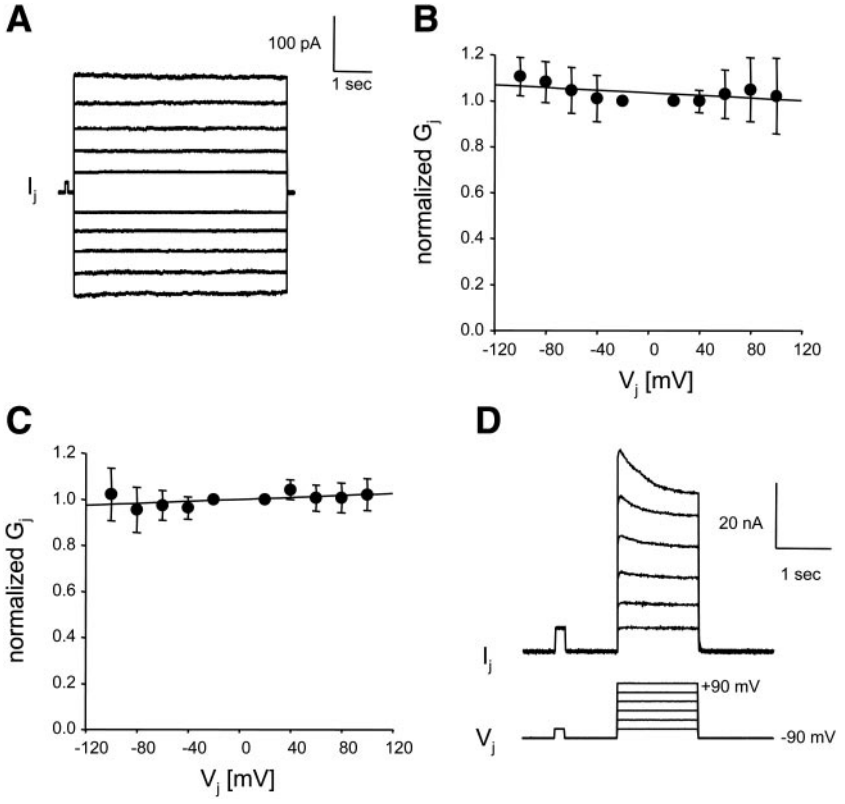

Fig. 5. Intercellular channels formed by Cx31.9 exhibit an exceptionally high voltage-gating threshold. *A*: junctional currents (I_j) recorded from transfected N2A cells in response to transjunctional voltage (V_j) steps of opposite polarity applied in 20-mV increments up to ±100 mV. *B*: plot of the relationship of V_j to steady-state G_j normalized to the values obtained at ±20 mV. No significant effect of voltage on channel conductance was observed in N2A cells. *C*: plot of the Cx31.9 G_j/V_j relationship obtained in paired *Xenopus* oocytes normalized to the values obtained at ±20 mV. Like N2A cells, voltage gating was not observed in oocyte pairs at V_j values up to ±100 mV. *D*: family of I_js recorded from an oocyte pair in response to V_j steps up to +180 mV applied in 30-mV increments. At supraphysiological values of V_j (≥150 mV), I_j values declined slightly. A short depolarizing step of 30 mV was applied between sweeps to ensure that G_j remained stable during the test. This trace is representative of three others. Straight lines in *B* and *C* represent linear regression fits with intercept near unity and negligible slope. Results in *B* and *C* are means ± SE of 4 N2A pairs and 13 oocyte pairs, respectively.

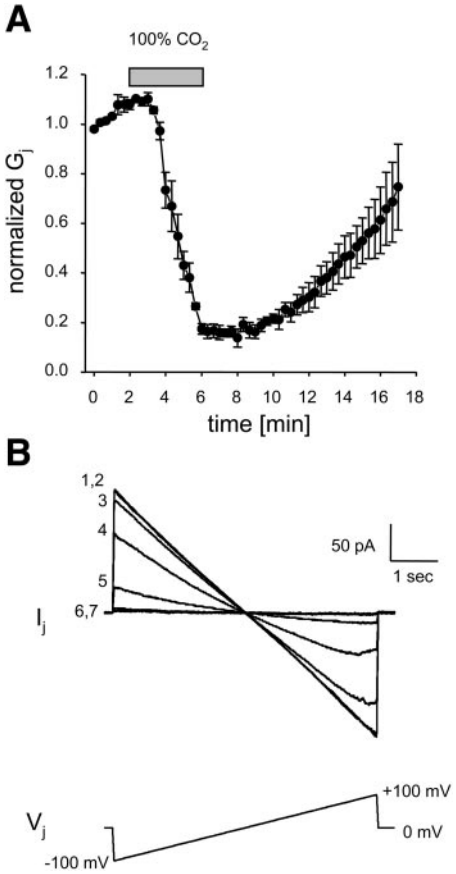

Fig. 6. Pharmacological inhibition of Cx31.9 channels. *A*: oocyte pairs expressing Cx31.9 were perfused with modified Barth's (MB) solution equilibrated with 100% CO_2 for 4 min (shaded bar), after which the perfusion medium was switched back to normal MB to allow G_j to recover. G_j was normalized to the average conductance values recorded during the first minute of the experiment. Results are means ± SE of 3 pairs. *B*: a Cx31.9-transfected N2A cell pair with 1.7 nS of initial conductance was exposed to 4 mM halothane. During 7 successive sweeps of a 7.7-s ramp protocol that varied the applied voltage from −100 to +100 mV, I_j decreased ≥99% within 1 min. Data are representative of 2 additional experiments.

lular currents from a Cx31.9-expressing N2A-cell pair with 1.7 nS of initial conductance. Seven successive sweeps of a 7.7-s ramp protocol that varied the applied voltage from −100 to +100 mV are illustrated. Application of 4 mM halothane at the onset of *sweep 1* resulted in a 99% decrease in I_j with 1 min. Junctional conductance recovered rapidly on halothane washout (not shown). These data show that despite the absence of a physiologically relevant voltage gate, Cx31.9 channels were endowed with chemical gating mechanisms indistinguishable from those of other members of the connexin family.

Unitary conductance of Cx31.9 channels. We routinely failed to observe current transitions between open and closed states of Cx31.9 channels at V_j values up to ±120 mV in N2A cell pairs. The absence of Cx31.9 voltage gating within this physiological range suggested that this result could be due to the channels residing predominantly in the open state. Alternatively, Cx31.9 channels might have a very small unitary conductance (γ_j) with transitions that would be poorly resolved at these voltages. To further examine this issue, we performed a limited series of experiments where supraphysiological driving voltages were applied to Cx31.9 cell pairs that displayed low levels of coupling. Figure 7 shows two representative traces derived from cell pairs that contain two active gap junction channels. At a V_j of 160 mV, both channels remained open for most of the duration of the pulse with one channel closing briefly (Fig. 7*A*). In a second trace acquired at 140 mV, one of the two channels transited to the closed state twice during the voltage pulse (Fig. 7*B*). Because such transitions were only rarely observed, we were unable to obtain sufficient data to accurately calculate either open probability or values of γ_j. We did qualitatively measure γ_j in all traces where clear transitions could be resolved, and we consistently obtained values between 12 and 15 pS (in 130 mM CsCl, Fig. 7*C*). Thus Cx31.9 appears to form channels with a relatively low γ_j value that remain predominantly open at physiological voltages.

Comparison of Cx31.9 and XenCx38 voltage gating. Several studies using both oocyte pairs and transfected cells have documented that connexons do not invari-

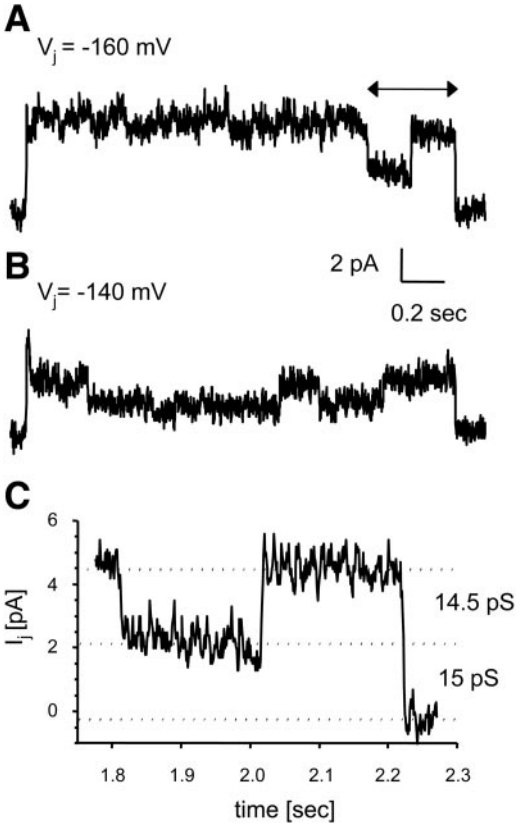

Fig. 7. Unitary conductance (γ_j) of Cx31.9 channels. Discrete current transitions were infrequently resolved only at V_j values >120 mV. *A*: unitary current transitions measured at a V_j of −160 mV in a cell pair that displayed 30 pS of total conductance. *B*: at a V_j of −140 mV, one of the two channels present in the recording gated to the closed state twice during the voltage pulse. *C*: expanded portion (arrow) of the trace shown in *A*. Qualitative measurement of γ_j in the two conducting states yielded γ_j values of ~15 pS (in 130 mM CsCl), which suggests that two channels were present.

ably maintain their electrical "fingerprints" when they pair heterotypically with a different connexon; thus distinct functional properties may arise from connexon-connexon interactions in heterotypic channels (37). Heterotypic pairing of Cx31.9 to XenCx38 offered a unique possibility to evaluate whether altered gating properties would result from interactions between voltage-sensitive XenCx38 and voltage-insensitive Cx31.9 connexons. As previously reported (7, 13), coupling between homotypic pairs of oocytes that expressed XenCx38 displayed a marked sensitivity to voltage with symmetrical decreases of I_j at V_j values greater than ±20 mV (Fig. 8*A*). Furthermore, the plot of G_{jss} versus V_j (Fig. 8*B*) confirmed that the voltage-dependent component of XenCx38 gating could not be precisely fit by a simple Boltzmann equation (7, 43). In contrast, analysis of heterotypic Cx31.9/XenCx38 I_js showed a clear asymmetric voltage closure with the XenCx38 side closing for V_j values >40 mV, whereas the Cx31.9 side was unaffected by voltage (Fig. 8*C*). Plotting the G_j/V_j relationship revealed a slight reduction in the G_{jss} value when the Cx31.9 side of the channel was relatively positive with regard to V_j, albeit ≥90% of the initial conductance remained at the largest V_j value tested (120 mV, Fig. 8*D*). This deviation from the behavior of homotypic Cx31.9 channels could represent either a novel property imparted by the allosteric interaction of Cx31.9 with a highly voltage-gated connexon or alternatively could result from a minimal contribution of homotypic XenCx38 channels that escaped antisense blockade.

Closer inspection of the heterotypic currents when the XenCx38 side was relatively positive revealed two additional interesting features of the Cx31.9/XenCx38 interaction: changes in both the voltage sensitivity and in the kinetics of channel closure. First, whereas XenCx38 remained voltage sensitive even when paired to Cx31.9, there was an obvious shift in the threshold of voltage gating as currents began to decline only for V_j values >40 mV. In fact, all parameters that describe the voltage gating behavior of XenCx38 were almost identical for both homotypic and heterotypic pairs except for the V_j required to elicit a conductance midway between G_{jmax} and G_{jmin} (V_0), which was markedly shifted to higher values (Table 1).

Second, analysis of the kinetics of channel closure revealed that XenCx38 connexons gated more slowly when heterotypically paired to Cx31.9, despite the fact that at equilibrium the current decay resulted in comparable values of G_{jmin} for either homotypic XenCx38 or heterotypic Cx31.9/XenCx38 intercellular channels (see Fig. 8*D*, Table 1). A representative example of fits of homotypic and heterotypic XenCx38 current decays in response to V_j steps of +80 and +100 mV are shown in Fig. 9. In the case of homotypic XenCx38/XenCx38 channels, the mean τ values were 0.203 ± 0.014 and

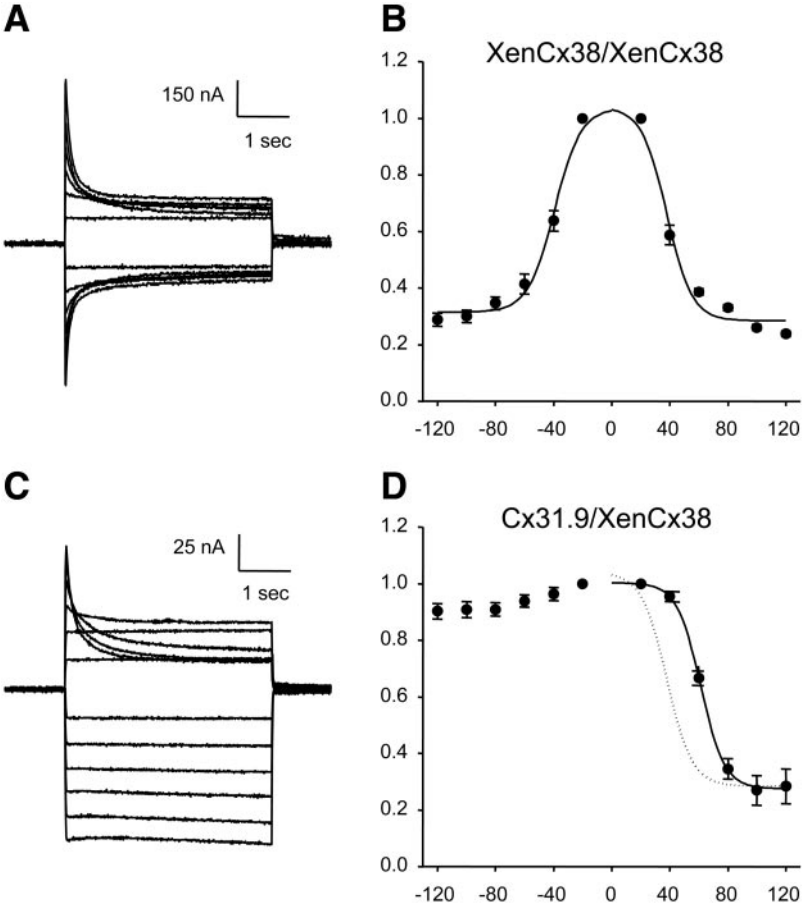

Fig. 8. Cx31.9 forms asymmetrically voltage-gated heterotypic channels with XenCx38. Oocytes were injected either with antisense oligonucleotides and Cx31.9 or were mock treated with water to retain expression of the endogenous connexin (XenCx38). *A*: I_j values from homotypic XenCx38 pairs recorded in response to V_j steps of opposite polarity applied in 20-mV increments. Currents declined toward nonzero steady-state levels for polarizing steps greater than ±20 mV as expected for intercellular channels composed of XenCx38. *B*: plot of the relationship of V_j to G_j normalized to the values obtained at ±20 mV for XenCx38. *C*: in contrast, heterotypic Cx31.9/XenCx38 currents exhibited a highly asymmetric voltage dependence with virtually no gating when the Cx31.9 cell was relatively positive, whereas the XenCx38 side exhibited a time-dependent channel closure at V_j values >40 mV. *D*: plot of the G_j/V_j relationship for heterotypic channels. V_j is defined as positive for depolarization and as negative for hyperpolarization of the XenCx38 cell relative to the Cx31.9 cell. Solid lines represent the best fits to Boltzmann equations for which the parameters are given in Table 1. Dashed line in *D* represents the superimposed Boltzmann fit for homotypic XenCx38 channels shown in *B*. Results are shown as means ± SE of 10–11 pairs.

Table 1. *Boltzmann parameters of intercellular channels composed of connexin31.9 and Xenopus connexin38*

Channel	V_j	G_{jmax}	G_{jmin}	A	n	V_0, mV
XenCx38/XenCx38	+	1	0.28	0.12	2.9	38
XenCx38/XenCx38	−	1	0.31	0.11	2.7	39
Cx31.9/XenCx38	+	1	0.23	0.12	2.9	62
Cx31.9/XenCx38	−	ND	ND	ND	ND	ND

Junctional conductance (G_j) developed between pairs of *Xenopus laevis* oocytes in response to increasing transjunctional potentials (V_j) was normalized to conductance measured at a V_j of ±20 mV (G_{jmax}, set as unity). Data were fit to the Boltzmann equation described in MATERIALS AND METHODS. Cooperativity constant A reflects channel voltage sensitivity and can also be expressed as equivalent number (n) of electron charges moving through transjunctional voltage field. Homotypic channels composed of connexin31.9 (Cx31.9) exhibited no voltage gating in physiological range; therefore Boltzmann parameters could not be determined. Signs + and − for V_j refer to transjunctional potential polarity. In heterotypic channels, $+V_j$ denotes XenCx38 oocyte is relatively positive, whereas $-V_j$ denotes Cx31.9 injected cell is relatively positive. These parameters were derived from oocyte pairs with G_j values (means ± SE) of 3.9 ± 1.2 μS (n = 10) for XenCx38/XenCx38 and 0.8 ± 0.1 μS (n = 11) for Cx31.9/XenCx38. G_{jmin}, minimum conductance value as estimated from Boltzmann fit; V_0, voltage at which half-maximal decrease of G_j is measured; ND, not determined.

0.162 ± 0.009 s for V_j values of +80 (n = 8) and +100 mV (n = 8), respectively. When XenCx38 was heterotypically paired to Cx31.9, τ values were significantly slower ($P \leq 0.001$), averaging 0.364 ±0.011 and 0.251 ±0.006 s for depolarizing steps of +80 (n = 8) and +100 mV (n = 8), respectively. Thus interactions of the voltage-gated XenCx38 connexons with the voltage-insensitive Cx31.9 connexons produced notable reductions in both the threshold and rate of XenCx38 voltage-dependent closure.

DISCUSSION

We have identified and functionally characterized a new member of the human connexin gene family, Cx31.9. The Cx31.9 sequence clustered within a subgroup of connexins distinct from the previously described α- or β-subfamilies (19). Cx31.9 mRNA was distributed in the brain and several other organs and was present in the human EST database. In two different functional expression assays, Cx31.9 formed intercellular channels that were distinguished by a low γ_j and a remarkable insensitivity to V_j. Thus Cx31.9 represents a novel human connexin that forms channels with unique functional properties.

The new human Cx31.9 gene is closely related to the human Cx32.4 gene with which it shares 76% sequence identity and localization on chromosome 17. Of all other connexin genes, only connexin26 and connexin30, which also reside on the same chromosome (human 13, mouse 14), share as high a level of amino acid identity (10, 18). The main differences between Cx31.9 and Cx32.4 are an 18-amino acid insertion into the cytoplasmic loop of Cx31.9 and a general loss of homology in the second half of the cytoplasmic tail including the absence of the proline-rich domain in Cx32.4. Thus it appears that the Cx31.9 and Cx32.4 genes may have arisen by gene duplication.

The dendrogram of all known human connexin sequences (see Fig. 2) supports the idea of a common origin for these genes and their assignment to a third subgroup distinct from the α- or β- connexin genes. Many reports had previously noted that the sequence divergence between connexin36 (Cx36) or connexin45 (Cx45) and the α-connexins was greater than the sequence divergence between the α- and β-subfamilies themselves (2, 6, 22, 23, 28). Despite this, Cx45 (vari-

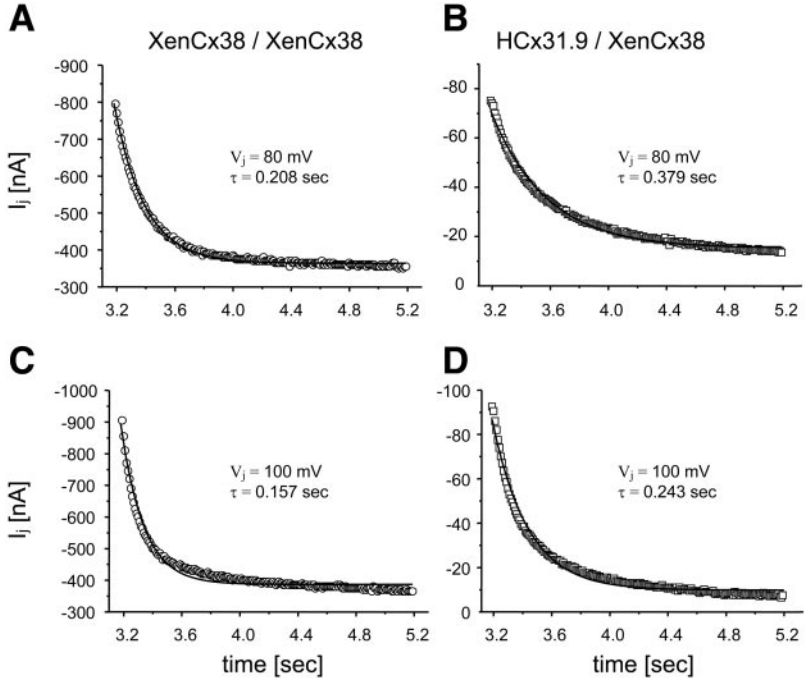

Fig. 9. Cx31.9 slows the kinetics of voltage-dependent closure of XenCx38 in heterotypic channels. For all data sets, the time-dependent decline in I_j was well fit by a single exponential function (solid lines) where time constant (τ) values decreased with increasing driving force. Values of τ for homotypic XenCx38 channels (A and B, ○) were markedly and significantly faster than for heterotypic Cx31.9/XenCx38 channels when the XenCx38 cell was depolarized (C and D, □). Traces are representative of 7 others; mean τ values are given in the text.

ously called either α-6 or α-7) and Cx36 (α-9) were erroneously assigned to the α-subgroup (20). Our analysis clearly indicates the existence of a third subfamily that is equal in magnitude to the previously described groups. It should be noted that the original division into two groups has always been poorly defined (17, 19), and an alternative view would be that there is simply one broad family of connexin genes.

Several observations suggested that Cx31.9 was a functional member of the connexin family. First, the Cx31.9 sequence displayed features consistent with other well-characterized connexins, including four potential transmembrane domains and conserved extracellular cysteine residues required for hemichannel docking (11). Second, transcription of the Cx31.9 gene has been confirmed by RT-PCR analysis and a search of the human EST database. Finally, when Cx31.9 was expressed in *Xenopus* oocytes or N2A cells, it formed gap junction channels that lacked voltage dependence but retained normal chemical gating, which indicates that the two gates were independent. This observation was in keeping with previous studies that have used chimerical constructs and connexin mutants to show that the two mechanisms could be independently modulated (33, 35). Taken together, these data demonstrate that Cx31.9 is an actively transcribed and functional connexin.

Heterotypic pairing of Cx31.9 to XenCx38 offered a unique opportunity to evaluate alterations in gating properties that result from interactions between voltage-sensitive and -insensitive connexons. In light of the fact that Cx31.9 did not display physiologically relevant voltage gating, it was surprising to find that the voltage-gating threshold and kinetics of XenCx38 shifted when it was paired with Cx31.9 in heterotypic channels. Historically, V_j sensitivity of gap junctional channels was considered an intrinsic property of the component hemichannels (4, 5, 14, 15). However, in many examples, connexins did not invariably maintain electrical fingerprints when paired with a different partner, and these distinct gating properties may have arisen from connexon-connexon interactions in heterotypic channels (7, 16, 38, 39). Our data indicate that the voltage-insensitive Cx31.9 imparted a higher voltage threshold to XenCx38 connexons that also gated with much slower τ values.

The absence of voltage sensitivity in Cx31.9 may be a reflection of the unusually high proline content of this connexin (11%) relative to voltage-sensitive connexins like XenCx38 (5% proline, 17 of 334 amino acids). The high proline content of Cx31.9 might result in a more rigid structure that is incapable of undergoing the conformational changes associated with gating at physiological voltages. It is not clear how pairing the insensitive Cx31.9 with XenCx38 resulted in a >20 mV shift in the voltage-gating threshold and a significant slowing of the kinetics of channel closure. The number of predicted gating charges did not change between heterotypic and homotypic channels when the XenCx38 side was positive, which is consistent with conservation of this property in the heterotypic channels. Further studies are required to elucidate the exact mechanisms by which Cx31.9 is able to modulate the voltage gating of XenCx38. Finally, this unique characteristic of Cx31.9 offers a novel approach to future mutational analysis of gap junction gating by screening for amino acid substitutions that will introduce voltage sensitivity.

We thank M.-M. Gabellec for excellent technical assistance.

This study was supported by funding from National Institutes of Health Grants EY-13163, AR-47102, and DC-005491 (to T. W. White); EY-013869 (to M. Srinivas); EY-06516 (to H. Ripps); the Telethon Foundation Grant E.1283 and the Italian Ministero dell' Università e della Ricerca Scientifica e Tecnologica (to D. F. Condorelli); the Association RETINA France (to R. Bruzzone); and by fellowships from the Marine Biological Laboratory at Woods Hole, MA (to T. W. White, M. Srinivas, and R. Bruzzone).

REFERENCES

1. **Barrio LC, Suchyna T, Bargiello T, Xu LX, Roginski RS, Bennett MV, and Nicholson BJ.** Gap junctions formed by connexins 26 and 32 alone and in combination are differently affected by applied voltage. *Proc Natl Acad Sci USA* 88: 8410–8414, 1991.
2. **Belluardo N, Trovato-Salinaro A, Mudo G, Hurd YL, and Condorelli DF.** Structure, chromosomal localization, and brain expression of human Cx36 gene. *J Neurosci Res* 57: 740–752, 1999.
3. **Beyer EC and Willecke K.** Gap junction genes and their regulation. In: *Gap Junctions*, edited by Hertzberg EL. Stamford, CT: Jai, 2000, p. 1–30.
4. **Brink P.** Gap junction voltage dependence: a clear picture emerges. *J Gen Physiol* 116: 11–12, 2000.
5. **Bruzzone R, Haefliger JA, Gimlich RL, and Paul DL.** Connexin40, a component of gap-junctions in vascular endothelium, is restricted in its ability to interact with other connexins. *Mol Biol Cell* 4: 7–20, 1993.
6. **Bruzzone R, White TW, and Goodenough DA.** The cellular Internet: on-line with connexins. *Bioessays* 18: 709–718, 1996.
7. **Bruzzone R, White TW, and Paul DL.** Expression of chimeric connexins reveals new properties of the formation and gating behavior of gap junction channels. *J Cell Sci* 107: 955–967, 1994.
8. **Bruzzone R, White TW, and Paul DL.** Connections with connexins: the molecular basis of direct intercellular signaling. *Eur J Biochem* 238: 1–27, 1996.
9. **Burt JM and Spray DC.** Volatile anesthetics block intercellular communication between neonatal rat myocardial cells. *Circ Res* 65: 829–837, 1989.
10. **Dahl E, Manthey D, Chen Y, Schwarz HJ, Chang YS, Lalley PA, Nicholson BJ, and Willecke K.** Molecular cloning and functional expression of mouse connexin-30, a gap junction gene highly expressed in adult brain and skin. *J Biol Chem* 271: 17903–17910, 1996.
11. **Dahl G, Werner R, Levine E, and Rabadan-Diehl C.** Mutational analysis of gap junction formation. *Biophys J* 62: 172–180, 1992.
12. **Delmar M, Morley GE, and Taffet SM.** Molecular analysis of the pH regulation of the cardiac gap junction protein connexin43. In: *Discontinuous Conduction in the Heart*, edited by Spooner PM, Joyner RW, and Jalife J. Armonk, NY: Futura, 1997, p. 203–221.
13. **Ebihara L, Beyer EC, Swenson KI, Paul DL, and Goodenough DA.** Cloning and expression of a *Xenopus* embryonic gap junction protein. *Science* 243: 1194–1195, 1989.
14. **Harris AL.** Emerging issues of connexin channels: biophysics fills the gap. *Q Rev Biophys* 34: 325–472, 2001.
15. **Hennemann H, Suchyna T, Lichtenberg-Frate H, Jungbluth S, Dahl E, Schwarz J, Nicholson BJ, and Willecke K.** Molecular cloning and functional expression of mouse con-

nexin40, a second gap junction gene preferentially expressed in lung. *J Cell Biol* 117: 1299–1310, 1992.
16. **Hopperstad MG, Srinivas M, and Spray DC.** Properties of gap junction channels formed by Cx46 alone and in combination with Cx50. *Biophys J* 79: 1954–1966, 2000.
17. **Hsieh CL, Kumar NM, Gilula NB, and Francke U.** Distribution of genes for gap junction membrane channel proteins on human and mouse chromosomes. *Somat Cell Mol Genet* 17: 191–200, 1991.
18. **Kelley PM, Abe S, Askew JW, Smith SD, Usami S, and Kimberling WJ.** Human connexin 30 (GJB6), a candidate gene for nonsyndromic hearing loss: molecular cloning, tissue-specific expression, and assignment to chromosome 13q12. *Genomics* 62: 172–176, 1999.
19. **Kumar NM and Gilula NB.** Molecular biology and genetics of gap junction channels. *Semin Cell Biol* 3: 3–16, 1992.
20. **Lo CW.** Genes, gene knockouts, and mutations in the analysis of gap junctions. *Dev Genet* 24: 1–4, 1999.
21. **Methfessel C, Witzemann V, Takahashi T, Mishina M, Numa S, and Sakmann B.** Patch clamp measurements on *Xenopus laevis* oocytes: currents through endogenous channels and implanted acetylcholine receptor and sodium channels. *Pflügers Arch* 407: 577–588, 1986.
22. **O'Brien J, Al Ubaidi MR, and Ripps H.** Connexin 35: a gap-junctional protein expressed preferentially in the skate retina. *Mol Biol Cell* 7: 233–243, 1996.
23. **O'Brien J, Bruzzone R, White TW, Al Ubaidi MR, and Ripps H.** Cloning and expression of two related connexins from the perch retina define a distinct subgroup of the connexin family. *J Neurosci* 18: 7625–7637, 1998.
24. **Plum A, Hallas G, Magin T, Dombrowski F, Hagendorff A, Schumacher B, Wolpert C, Kim J, Lamers WH, Evert M, Meda P, Traub O, and Willecke K.** Unique and shared functions of different connexins in mice. *Curr Biol* 10: 1083–1091, 2000.
25. **Rozental R, Srinivas M, and Spray DC.** How to close a gap junction channel. Efficacies and potencies of uncoupling agents. *Methods Mol Biol* 154: 447–476, 2001.
26. **Simon AM and Goodenough DA.** Diverse functions of vertebrate gap junctions. *Trends Cell Biol* 8: 477–483, 1998.
27. **Skerrett IM, Merritt M, Zhou L, Zhu H, Cao F, Smith JF, and Nicholson BJ.** Applying the *Xenopus* oocyte expression system to the analysis of gap junction proteins. *Methods Mol Biol* 154: 225–249, 2001.
28. **Sohl G, Degen J, Teubner B, and Willecke K.** The murine gap junction gene connexin36 is highly expressed in mouse retina and regulated during brain development. *FEBS Lett* 428: 27–31, 1998.
29. **Spray DC, Harris AL, and Bennett MV.** Equilibrium properties of a voltage-dependent junctional conductance. *J Gen Physiol* 77: 77–93, 1981.
30. **Thompson JD, Higgins DG, and Gibson TJ.** CLUSTAL W: improving the sensitivity of progressive multiple sequence alignment through sequence weighting, position-specific gap penalties, and weight matrix choice. *Nucleic Acids Res* 22: 4673–4680, 1994.
31. **Turner DL and Weintraub H.** Expression of achaete-scute homolog 3 in *Xenopus* embryos converts ectodermal cells to a neural fate. *Genes Dev* 8: 1434–1447, 1994.
32. **Veenstra RD.** Determining ionic permeabilities of gap junction channels. *Methods Mol Biol* 154: 293–311, 2001.
33. **Wang XG and Peracchia C.** Connexin 32/38 chimeras suggest a role for the second half of inner loop in gap junction gating by low pH. *Am J Physiol Cell Physiol* 271: C1743–C1749, 1996.
34. **Wang XG and Peracchia C.** Positive charges of the initial C-terminus domain of Cx32 inhibit gap junction gating sensitivity to CO_2. *Biophys J* 73: 798–806, 1997.
35. **Wang XG and Peracchia C.** Molecular dissection of a basic COOH-terminal domain of Cx32 that inhibits gap junction gating sensitivity. *Am J Physiol Cell Physiol* 275: C1384–C1390, 1998.
36. **White TW.** Unique and redundant connexin contributions to lens development. *Science* 295: 319–320, 2002.
37. **White TW and Bruzzone R.** Multiple connexin proteins in single intercellular channels: connexin compatibility and functional consequences. *J Bioenerg Biomembr* 28: 339–350, 1996.
38. **White TW, Bruzzone R, Goodenough DA, and Paul DL.** Voltage gating of connexins. *Nature* 371: 208–209, 1994.
39. **White TW, Bruzzone R, Wolfram S, Paul DL, and Goodenough DA.** Selective interactions among the multiple connexin proteins expressed in the vertebrate lens—the second extracellular domain is a determinant of compatibility between connexins. *J Cell Biol* 125: 879–892, 1994.
40. **White TW and Paul DL.** Genetic diseases and gene knockouts reveal diverse connexin functions. *Annu Rev Physiol* 61: 283–310, 1999.
41. **White TW, Paul DL, Goodenough DA, and Bruzzone R.** Functional analysis of selective interactions among rodent connexins. *Mol Biol Cell* 6: 459–470, 1995.
42. **Wilders R and Jongsma HJ.** Limitations of the dual voltage clamp method in assaying conductance and kinetics of gap junction channels. *Biophys J* 63: 942–953, 1992.
43. **Willecke K, Heynkes R, Dahl E, Stutenkemper R, Hennemann H, Jungbluth S, Suchyna T, and Nicholson BJ.** Mouse connexin37: cloning and functional expression of a gap junction gene highly expressed in lung. *J Cell Biol* 114: 1049–1057, 1991.